Voltage-controlled Gating at the Intracellular Entrance to a Hyperpolarization-activated Cation Channel

Brad S. Rothberg, Ki Soon Shin, Prashant S. Phale, and Gary Yellen

Department of Neurobiology, Harvard Medical School, Boston, MA 02115

ABSTRACT Hyperpolarization-activated cation (HCN) channels regulate pacemaking activity in cardiac cells and neurons. Our previous work using the specific HCN channel blocker ZD7288 provided evidence for an intracellular activation gate for these channels because it appears that ZD7288, applied from the intracellular side, can enter and leave HCN channels only at voltages where the activation gate is opened (Shin, K.S., B.S. Rothberg, and G. Yellen. 2001. *J. Gen. Physiol.* 117:91–101). However, the ZD7288 molecule is larger than the Na^+ or K^+ ions that flow through the open channel. In the present study, we sought to resolve whether the voltage gate at the intracellular entrance to the pore for ZD7288 also can be a gate for permeant ions in HCN channels. Single residues in the putative pore-lining S6 region of an HCN channel (cloned from sea urchin; spHCN) were substituted with cysteines, and the mutants were probed with Cd^{2+} applied to the intracellular side of the channel. One mutant, T464C, displayed rapid irreversible block when Cd^{2+} was applied to opened channels, with an apparent blocking rate of $\sim 3 \times 10^5$ $M^{-1}s^{-1}$. The blocking rate was decreased for channels held at more depolarized voltages that close the channels, which is consistent with the Cd^{2+} access to this residue being gated from the intracellular side of the channel. 464C channels could be recovered from Cd^{2+} inhibition in the presence of a dithiol applied to the intracellular side. The rate of this recovery also was reduced when channels were held at depolarized voltages. Finally, Cd^{2+} could be trapped inside channels that were composed of WT/464C tandem-linked subunits, which could otherwise recover spontaneously from Cd^{2+} inhibition. Thus, Cd^{2+} escape is also gated at the intracellular side of the channel. Together, these results are consistent with a voltage-controlled structure at the intracellular side of the spHCN channel that can gate the flow of cations through the pore.

KEY WORDS: HCN • SPIH • gating • Cd^{2+} • cysteine mutagenesis

INTRODUCTION

Hyperpolarization-activated cation (HCN)* current (termed I_f, I_h, or I_q) contributes to the generation of spontaneous rhythmic activity in the heart and brain (Brown et al., 1979; Brown and DiFrancesco, 1980; Pape and McCormick, 1989; for reviews see DiFrancesco, 1993; Pape, 1996). The family of channels that produce these currents, known as HCN channels, has been cloned from mammalian tissues (Ludwig et al., 1998; Santoro et al., 1998). These channels are related to depolarization-activated K^+ channels (K_V channels), with six putative transmembrane domains. HCN channels also contain a cyclic nucleotide binding domain, similar to that of CNG channels, which is consistent with the direct modulation of native I_f by intracellular cAMP (DiFrancesco and Tortora, 1991). One HCN homologue cloned from sea urchin, known as spHCN (or SPIH), shows some unique activation properties (Gauss et al., 1998). In the absence of cAMP, spHCN channels mediate a current that rapidly inactivates. Increasing cAMP abolishes this inactivation, resulting in voltage activation properties that are quite similar to those of mammalian HCNs. Despite our knowledge of the voltage- and cAMP-dependent behavior of these channels, the molecular basis of HCN channel gating is yet unclear.

Shin et al. (2001) demonstrated that the HCN channel blocker ZD7288 applied to the intracellular side blocks spHCN and mHCN1 channels rapidly at hyperpolarized voltages that open the channels, and more slowly at depolarized potentials that decrease the open probability. Also, in a triple point mutant channel that imparts the rapid voltage activation properties of spHCN to mHCN1, ZD7288 could be trapped in the channel by holding the blocked channel at a depolarized voltage. Together, these observations provide evidence for an intracellular activation gate because it appears that ZD7288, applied to the intracellular side of the channel, can enter and leave the pore only at voltages where the activation gate is opened. However, the ZD7288 mole-

The present address of P.S. Phale is Biotechnology Center, Indian Institute of Technology, Powai, Mumbai, 400 076, India.

Address correspondence to Dr. Gary Yellen, Department of Neurobiology, Harvard Medical School, 220 Longwood Avenue, Boston, MA 02115. Fax: (617) 432-0121; E-mail: gary_yellen@hms.harvard.edu

Abbreviations used in this paper: DMPS, 2,3-dimercapto-1-propanesulfonate; HCN, hyperpolarization-activated cation; HEK293, human embryonic kidney 293; P_{open}, open probability; spHCN, sea urchin HCN.

cule is larger than the Na^+ or K^+ ions that flow through the open channel. Thus, the presumed gating structure at the intracellular mouth of the HCN channel pore, although small enough to exclude ZD7288, may possibly allow Na^+ or K^+ to flow freely, and the activation gate for permeant ions may be found elsewhere.

In the present study, we sought to resolve whether the voltage gate for permeant ions in HCN channels is at the intracellular entrance to the pore using Cd^{2+} as a molecular gating probe. Because Cd^{2+} is closer in size to Na^+ and K^+ than ZD7288, it may better distinguish the gate for permeant ions from structures that can occlude larger molecules from the pore. Our approach was to engineer a high affinity binding site for Cd^{2+} in the pore of the spHCN channel using cysteine mutagenesis of residues in the pore-lining S6 region (Liu et al., 1997). One such high affinity mutant was found at spHCN position 464. Currents through the mutant T464C channel were blocked irreversibly by Cd^{2+} applied to the intracellular side of the channel. The apparent blocking rate could be slowed by holding the channel closed at depolarized voltages, which is consistent with an intracellular gate that could prevent Cd^{2+} access to 464. The current could be recovered by applying the dithiol reagent DMPS to hyperpolarized, but not depolarized, channels, which is further consistent with an intracellular gate that can prevent DMPS access (and Cd^{2+} exit) while the channel is closed. Finally, Cd^{2+} could be trapped inside channels that were composed of WT/464C tandem-linked subunits that could otherwise recover spontaneously from Cd^{2+} inhibition.

These results provide evidence for a voltage-controlled structure at the intracellular mouth of an HCN channel that can gate the flow of metal cations through the pore, implying that the voltage activation gate for HCN channels may have a similar architecture to that of *Shaker* voltage-gated K^+ channels (Liu et al., 1997; Yellen, 1998), but may be coupled to the voltage sensor differently. A preliminary report of these findings has appeared in Rothberg et al. (2001).

MATERIALS AND METHODS

Expression of Recombinant spHCN Channels

spHCN (SPIH) channels were transiently expressed in human embryonic kidney 293 cells (HEK 293; American Type Culture Collection) as described previously (Shin et al., 2001). As in our previous experiments, we used a modified "wild-type" spHCN channel with the mutation M349I (in the S4 region of spHCN) to increase functional expression levels while leaving the qualitative features of wild-type activation and deactivation intact. Cells were cotransfected with the πH3-CD8 plasmid (Seed and Aruffo, 1987), which expresses the α subunit of the human CD8 lymphocyte antigen. Cells expressing the CD8 antigen were identified by decoration with antibody-coated beads (Jurman et al., 1994).

Construction of Tandem Dimers and Site-directed Mutagenesis

Point mutations were introduced by PCR (Ausubel et al., 1996) and confirmed by sequencing. The tandem dimer construct was generated by eliminating the stop codon of the "A" protomer and inserting the "B" protomer cDNA using an introduced KpnI site in the pcDNA4 expression vector. The full-length dimer contained the 10–amino acid linker GSGGTELGST connecting the former COOH terminus of the A protomer with the initial methionine of the B protomer.

Solutions and Electrophysiological Recordings

All experiments were performed with excised inside-out patches (Hamill et al., 1981) from identified transfected cells 1–2 d after transfection. Experiments were done at room temperature (22–24°C). Currents were low-pass filtered at 1–2 kHz and digitized at 5–50 kHz. The recording and rapid perfusion switching methods have been described previously (Liu et al., 1997). Solutions bathing both sides of the membrane contained the following (in mM): 160 KCl, 0.5 $MgCl_2$, and 10 HEPES, pH 7.4. The solution at the extracellular face of the patch additionally contained 1 mM EGTA, whereas solutions at the intracellular face of the patch contained 100 μM cAMP and either 20 μM EGTA (control solution) or $CdCl_2$ with no EGTA (Cd^{2+} solution). Some experiments with the 459C mutant used the HCN channel blocker ZD7288 (Tocris) to distinguish between HCN current and endogenous background current. For experiments using 2,3-dimercapto-1-propanesulfonate (DMPS; Aldrich), the reagent was dissolved in intracellular solution containing 20 μM EGTA within a few minutes before use.

We observed a shift in the voltage activation midpoint ($V_{1/2}$) for spHCN channels toward negative potentials after patch excision, from around −50 mV immediately after excision to a stable level of around −65 mV that was reached ~4 min after excision; this was similar to the shift reported for mammalian HCN channels after patch excision (Chen et al., 2001a,b). Experiments for this paper were typically begun 3–4 min after excision, thus, we expect that this shift would have little effect on the results.

RESULTS

Cysteines in the S6 Region of an HCN Channel Can Form Binding Sites for Cd^{2+} that Block Current or Modify Gating

We introduced cysteines individually at 14 different positions along the S6 transmembrane region of the spHCN channel (positions 459–472), and initially examined the gating characteristics of the mutants in the presence of 100 μM cAMP to prevent inactivation (Gauss et al., 1998). Two of the mutants (463C and 469C) yielded no current when transfected into HEK293 cells. The gating of the 459C and 471C mutants showed a shift toward depolarized voltages, and closing was incomplete in the 459C mutant, even at +50 mV. In contrast, the gating of 465C was shifted slightly toward more hyperpolarizing voltages. The remaining 9 of the 14 mutants displayed gating that was similar to wild-type.

We tested the ability of each mutant to form a high affinity binding site for Cd^{2+} by applying 20 μM Cd^{2+} to the intracellular side of excised inside-out patches in the presence of 100 μM cAMP (Fig. 1). Little effect of

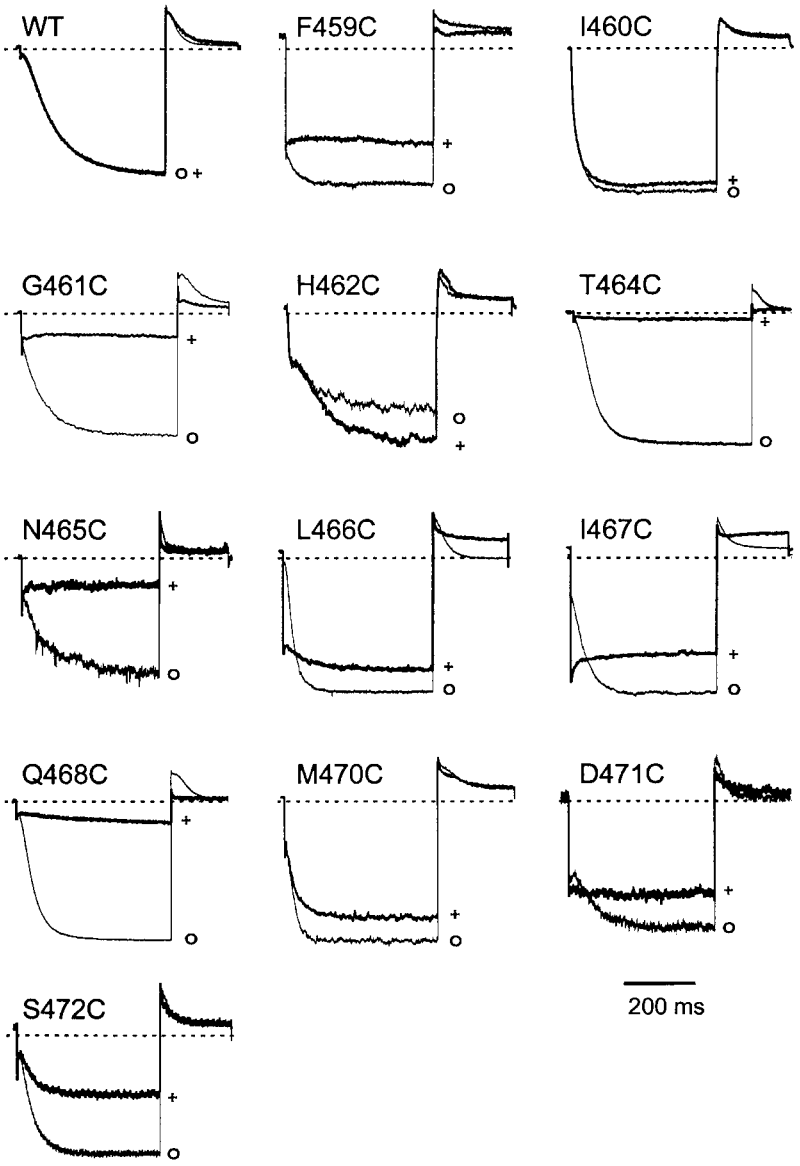

FIGURE 1. Effects of Cd^{2+} on wild-type and S6 cysteine-substituted spHCN channels. Representative recordings from inside-out patches excised from HEK293 cells expressing wild-type (WT) or mutant spHCN before (o) or during (+) application of 20 μM intracellular Cd^{2+}. Dashed lines represent zero current levels. Channels were held at +10 mV, and currents were elicited by a step to −110 mV, followed by a step to +30 mV. For 459C and D471C, channels were held at +50 mV and stepped to −90 mV, and then back to +50 mV. Currents were not leak-subtracted. Time scale bar (200 ms) applies to all currents except G461C (100 ms) and N465C (400 ms). Maximum inward currents for these traces: WT, 736 pA; F459C, 101 pA; I460C, 52 pA; G461C, 142 pA; H462C, 32 pA; T464C, 761 pA; N465C, 95 pA; L466C, 221 pA; I467C, 241 pA; Q468C, 826 pA; M470C, 178 pA; and S472C, 209 pA.

Cd^{2+} was seen for wild-type spHCN channels and the 460C mutant. Two other mutants (470C and 472C) showed moderate levels of inhibition (30–60%) in the presence of Cd^{2+}. Four mutants (459C, 466C, 467C, and 471C) showed moderate inhibition (20–50%) by Cd^{2+}, but also a prominent "lock-open" effect similar to that observed for the *Shaker* mutant 476C (Holmgren et al., 1998). Closing kinetics were markedly slowed in the presence of Cd^{2+}, and most or all time-dependent activation was replaced by an ohmic jump, representing current through channels that were chronically open. This effect was reversible upon washout of Cd^{2+}, although the inhibitory effects of Cd^{2+} on these mutants often showed little recovery. Finally, the 462C mutant showed potentiation of the current in the presence of Cd^{2+}, which also was rapidly reversible upon washout.

The remaining four mutants (461C, 464C, 465C, and 468C) were inhibited strongly (by >80%) in the presence of 20 μM intracellular Cd^{2+}. One of these, the 464C mutant, gave a particularly strong Cd^{2+} effect that was also irreversible. We focused on Cd^{2+} binding to this mutant to learn more about HCN channel gating.

Cd^{2+} Irreversibly Inhibits the 464C Mutant in the Open State

The effect of Cd^{2+} on this mutant was particularly potent (>95% inhibition with 20 μM Cd^{2+}), and did not recover even after pulsing to −110 mV for several minutes in the presence of 1 mM EGTA. The tight binding of Cd^{2+} in this mutant suggested that the Cd^{2+} might be coordinated by two or more cysteines, which may be positioned optimally facing the central axis of the pore to form a Cd^{2+} binding site.

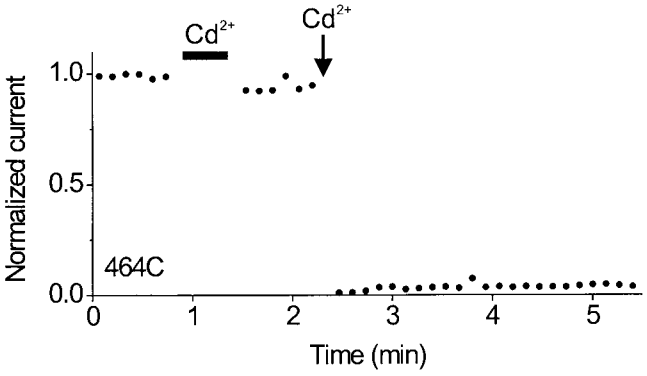

FIGURE 2. Cd^{2+} inhibits the 464C mutant rapidly only when the channels are open. Channels were held at +10 mV, and current was monitored using test pulses (400 ms) to −110 mV (closed circles). Cd^{2+} (20 μM, horizontal bar) was applied for 25 s to closed channels (at +10 mV), resulting in ~10% inhibition of current, which was irreversible. The same concentration of Cd^{2+} was then applied for 2 s to open channels (during a 5-s pulse to −110 mV, arrow), resulting in ~95% inhibition of current, which was also irreversible. Linear leak current was subtracted, and currents were normalized to the mean pre-Cd^{2+} control level.

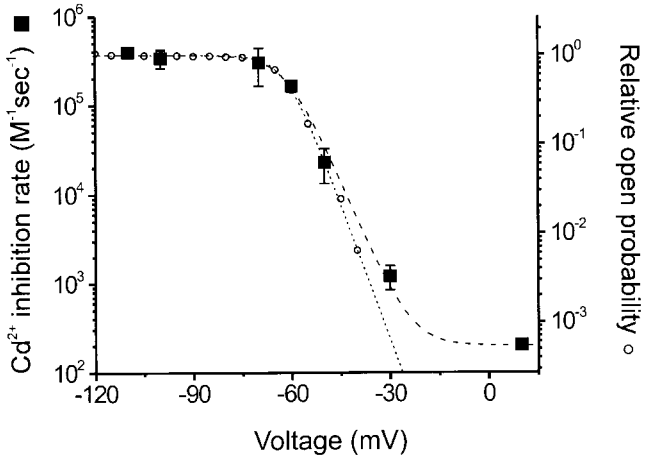

FIGURE 3. Voltage dependence of the Cd^{2+} inhibition rate of 464C channels. Rate constants (closed squares) are plotted as a function of voltage (means of three to five experiments at each voltage; bars indicate ±SEM). Relative open probabilities (open circles) obtained from tail current measurements are shown for comparison (means of five experiments). The dotted line is a Boltzmann function fit to the relative open probabilities, assuming that open probability goes to zero with increasing depolarization. The dashed line is a Boltzmann function fit with the Cd^{2+} inhibition rates, with a minimum rate of ~200 $M^{-1}s^{-1}$.

Cd^{2+} application to closed channels produced only a small (~10%) decrease in the current monitored by subsequent test pulses (Fig. 2). However, when Cd^{2+} was applied to the same patch for only 2 s while the channels were held open at −110 mV, the current was >95% inhibited. This experiment suggests that the cysteines at position 464 are accessible to Cd^{2+} from the intracellular side only while the channel is open.

If inhibition can only occur in open 464C channels, then the rate for Cd^{2+} inhibition should be correlated with the voltage dependence of channel open probability (P_{open}). We next measured the apparent blocking rates for Cd^{2+} at different voltages. For each voltage, we used repeated brief applications of Cd^{2+}, with intervening test pulses to −110 mV to monitor the reduction in current. The current remaining after each application was plotted as a function of cumulative Cd^{2+} application time to estimate the apparent rate constant at that voltage. The current decrease at each voltage was well described by a single exponential, which is consistent with inhibition of 464C channels by a single Cd^{2+}. The reciprocal of the time constant gives an apparent rate that varied linearly with [Cd^{2+}] (unpublished data), again consistent with the action of a single Cd^{2+}. This rate was divided by [Cd^{2+}] to give a second-order rate constant.

Fig. 3 shows that the rate constants plotted as a function of voltage correlated well with the relative P_{open} over the range of −110 to −30 mV. The binding of Cd^{2+} does not seem to have a large intrinsic voltage dependence because the inhibition rate constants for maximally opened channels was similar at different voltages (over the range of −70 to −110 mV; Fig. 3). At +10 mV, the inhibition rate was ~1,500-fold slower than the rate measured for maximally opened 464C channels. However, it was somewhat faster than that predicted by extrapolation of a simple Boltzmann fit if closed channels do not admit Cd^{2+} at all. This low rate at positive voltages may reflect the rate of Cd^{2+} entry into closed channels, or it may indicate that the P_{open} does not go to zero at these voltages (a limiting relative P_{open} of $\sim 6 \times 10^{-4}$ would explain the result). In either case, these results are consistent with the accessibility of Cd^{2+} to 464C being regulated by a voltage-dependent activation gate positioned intracellular to this residue.

Cd^{2+} Is Bound by at Least Three Cysteines in the Pore of the 464C Mutant

As mentioned above, the very tight binding of Cd^{2+} to the 464C mutant suggests the involvement of multiple cysteines. Because the channel is expressed as a homotetramer, all four of the introduced cysteines at position 464 can potentially contribute to the binding site, if it lies on the pore axis. To learn how many of these cysteines are involved, we expressed spHCN channels as tandem dimers that enabled some control over the stoichiometry of mutant residues.

We introduced the 464C mutation into one protomer in a tandem dimer construct; the other protomer contained the wild-type residue T464 (dimer TC). If channels are always formed by two tandem dimers (TC/TC), then these channels will contain two cysteines at 464 instead of four. In patches excised from cells transfected with the TC construct, 20 μM Cd^{2+} inhibited

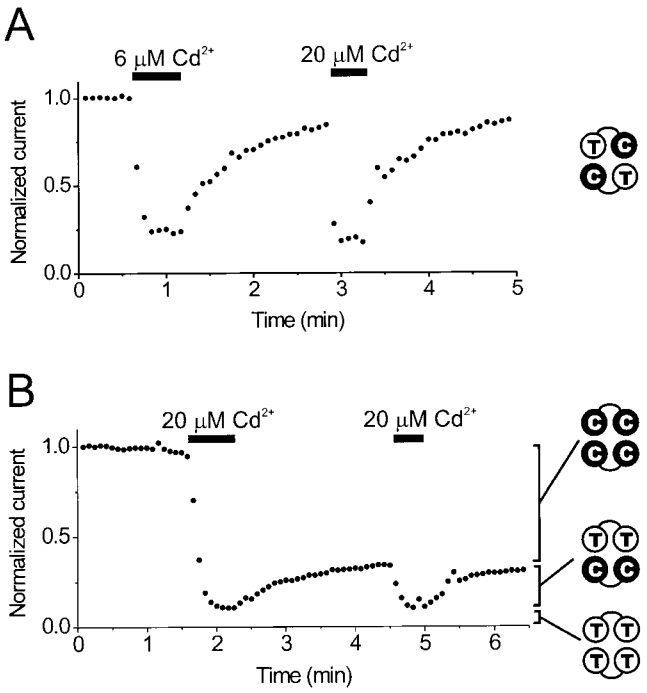

FIGURE 4. Cd^{2+} inhibition is reversible in channels containing only two cysteines at position 464. (A) Reversible Cd^{2+} inhibition in channels composed of TC tandem-linked subunit dimers (RESULTS). The TC/TC channels were ~80% inhibited in 6 μM Cd^{2+}, and the current recovered to near control levels in ~2 min. The channels were ~86% inhibited during a subsequent application of 20 μM Cd^{2+}. (B) Cd^{2+} inhibition in patches containing a mixture of channels composed of TT and CC dimers (RESULTS). In this experiment, the initial application of 20 μM Cd^{2+} inhibited ~90% of the current (CC/CC + TT/CC channels). Upon removal of Cd2+, ~25% of the current recovered in ~2 min (TT/CC channels). 65% of the current was blocked irreversibly (CC/CC channels). The recovered 25% could again be reversibly blocked by a subsequent application of 20 μM Cd^{2+}. The remaining 10% of the current was unaffected by Cd^{2+} (mostly TT/TT channels). For both A and B, channels were held at +10 mV, and current was monitored using 400-ms test pulses to −110 mV (closed circles). Linear leak current was subtracted, and currents were normalized to the mean pre-Cd^{2+} control level.

>80% of the current, but this effect was almost completely reversible upon washout (Fig. 4 A). This suggests that a channel containing two cysteines at 464 can be at least partially inhibited by Cd, but that two cysteines are not sufficient to bind Cd^{2+} irreversibly.

The majority of spHCN channels formed by two TC dimers probably contain cysteines at 464 in the two subunits diagonal from one another. Although these channels were not blocked irreversibly, two 464 cysteines, if they were located in adjacent subunits (closer to one another), might be sufficient for irreversible block. To test this possibility, we constructed one tandem dimer with cysteines at 464 in both protomers (CC) and another dimer composed of two wild-type protomers (TT). Cells containing both dimer constructs should contain a mixture of channels composed of either four wild-type subunits (TT/TT), four 464C subunits (CC/CC), or two wild-type and two 464C subunits (TT/CC). HEK293 cells were transfected with a mixture containing equal amounts of TT and CC expression plasmid. When expressed separately, the TT/TT channels are unaffected by Cd^{2+} and the CC/CC channels are completely and irreversibly inhibited by Cd^{2+} (not shown).

To test whether TT/CC channels are blocked reversibly or irreversibly, we first apply Cd^{2+} to achieve a maximal block of the mixture of channels. With the block at equilibrium, the remaining current should flow mainly through TT/TT channels. The patch is returned to the control solution. If no current recovers, this would suggest that two cysteines at 464 in adjacent subunits (as should be found in the TT/CC channels) are sufficient to bind Cd^{2+} irreversibly. In contrast, if some current recovers, this would suggest that two cysteines at 464 cannot form the irreversible Cd^{2+} binding site. What we see is that a portion of the current does recover upon washout (Fig. 4 B). Although the fraction of current that was reversibly inhibited by Cd^{2+} varied among cells, the proportions of reversible, partially reversible and irreversible current were consistent with a binomial distribution (Table I), suggesting that TT and CC dimers did combine with one another to form the predicted mixture of channels. Also, when cells were cotransfected with a 1:3 mixture of CC:TT expression plasmids, both the Cd^{2+}-insensitive fraction and the fraction of reversibly blocked current in the transfected

TABLE I

Predicted and Observed Fractions of Cd^{2+}-inhibited HCN Current with Mixed Tandem Dimers[a]

	Experiment			
	1	2	3	4
Transfected cDNA ratio (CC:TT)	1:1	1:1	1:3	1:1
Fraction irreversibly inhibited current	0.64	0.60	0.27	0.71
Inferred CC:TT dimer expression ratio[b]	4:1	3.3:1	1.1:1	5.3:1
Predicted fraction TT/TT channels[c]	0.04	0.05	0.23	0.025
Predicted fraction TT/CC channels[d]	0.32	0.35	0.50	0.265
Predicted fraction reversibly inhibited current[e]	0.27	0.30	0.42	0.23
Observed fraction reversibly inhibited current	0.25	0.20	0.39	0.21

[a]HEK293 cells were transfected with mixtures of TT and CC tandem dimer cDNAs, and the fraction of current inhibited reversibly and irreversibly by 20 μM Cd^{2+} was measured (Fig. 4 B). The current reversibly inhibited by Cd^{2+} is consistent with the predicted current through TT/CC channels.

[b]Estimated from the following: Fraction of CC subunits = (fraction irreversibly inhibited current)$^{0.5}$, and fraction of TT subunits = 1− fraction of CC subunits. The higher expression level estimated for CC relative to TT subunits is consistent with the typically larger currents we observed for CC/CC channels compared with TT/TT channels obtained with separate transfections.

[c](Fraction TT subunits)^2.

[d]1 − (Fraction irreversibly inhibited current) − (Predicted fraction TT/TT channels).

[e]We assume that 20 μM Cd^{2+} should inhibit only ~85% of the current through TT/CC channels, as it does for TC/TC channels (Fig. 4 A).

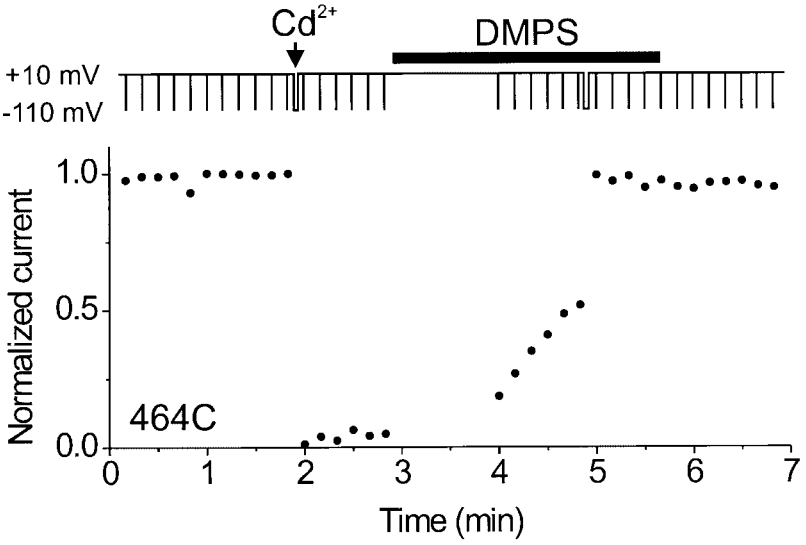

FIGURE 5. Recovery of Cd^{2+}-bound 464C channels is prevented by depolarization. 464C channels were held at +10 mV, and current was monitored using test pulses (400 ms) to −110 mV (closed circles). Channels were blocked with Cd^{2+} (20 μM, arrow) applied during a 5-s pulse to −110 mV. Little or no spontaneous recovery occurred with Cd^{2+} washout. DMPS (1 mM, horizontal bar) application was started while the channels were held at +10 mV. Little recovery was seen upon an initial test pulse in DMPS. Subsequent test pulses in DMPS speeded up recovery, and a long pulse (8 s) to −110 mV recovered the remaining blocked channels.

cells was increased. This was further consistent with the supposition that the reversibly blocked current is through TT/CC channels.

It seems that although two cysteines at 464 are sufficient to form a Cd^{2+} binding site, the binding is not irreversible, regardless of whether the cysteines are in adjacent or diagonal subunits. To produce irreversible Cd^{2+} inhibition, three or four cysteines at 464 are required. For these cysteines to coordinate a single Cd^{2+}, we must now assume that position 464 faces the central axis of the HCN channel pore. Cd^{2+} may inhibit current through these channels either by physically occluding the pore or by energetically stabilizing a closed conformation of the channel.

Is Access to 464C Controlled by an Activation Gate, or Do the 464 Cysteines Move Apart (or Become Buried) upon Closing?

The results of our dimer experiments, combined with the sharp voltage dependence of the Cd^{2+} blocking rate, suggest that Cd^{2+} can be coordinated by multiple cysteines near the central axis of the pore and that access to this binding site is governed by a voltage-dependent gate. However, it is also possible that the reduced binding of Cd^{2+} to closed channels occurs because the cysteines at 464 move apart from one another upon channel closing, leaving Cd^{2+} with no high affinity binding site. To distinguish between these possibilities, we used DMPS to facilitate Cd^{2+} release from blocked 464C channels. If access of DMPS to the binding site is impeded by a gate at depolarized voltages, then the current should recover more slowly at depolarized voltages than at hyperpolarized voltages. In contrast, if the cysteines move apart upon depolarization, then the current should recover more readily at depolarized voltages because the voltage-dependent movement of the cysteines should favor Cd^{2+} release. The experiment in Fig. 5 shows that in DMPS, the current recovers more slowly at depolarized voltages, which is consistent with access of DMPS being impeded by an intracellular gate when the channel is depolarized. This experiment further suggests that the gate of the channel is still somewhat functional, even when Cd^{2+} is bound.

Because the Cd^{2+}-bound channel's activation gate may be functional, it should be possible to further determine whether Cd^{2+} binding introduces a strong energetic bias toward either the open or closed state of the channel by measuring the rate of current recovery (i.e., Cd^{2+} release) in DMPS at different voltages. For example, if the positions of the cysteines are more optimal to coordinate Cd^{2+} while the channel is opened, then we might expect the voltage dependence of recovery to be strongly shifted toward more depolarized voltages because the closed state would be energetically unfavored in the Cd^{2+}-bound channel. Fig. 6 shows that a strong bias toward either the open or closed state is not introduced by Cd^{2+} binding. This suggests that the cysteines at position 464 do not move much during the gating process, despite their participation in the tight binding of Cd^{2+}. It also suggests that Cd^{2+} inhibits the current not by locking the gate closed, but rather by physically occluding the pore.

Can Cd^{2+} Be Trapped Inside a Closed Channel?

Although Cd^{2+} release from the 464C mutant in the presence of DMPS appears to be controlled by the voltage activation gate, it could still be argued that there is a gate that can exclude DMPS (a larger molecule than Cd^{2+}) but would allow Cd^{2+} to pass freely if it were not bound so tightly by the 464 cysteines. To test this, we used the WT/464C (TC) tandem dimer, which is reversibly blocked by Cd^{2+}, to perform a trapping experiment: we first block the channels with Cd^{2+}, and then

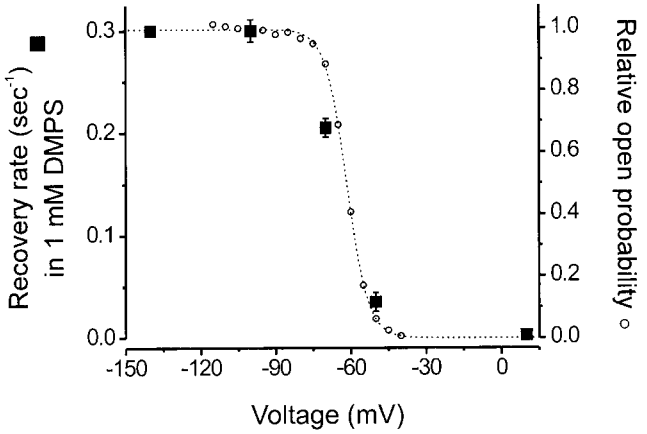

FIGURE 6. Voltage dependence of recovery rate for Cd^{2+}-bound 464C channels in the presence of 1 mM DMPS. Recovery rates (closed squares) are compared with relative open probabilities (open circles) for 464C channels. Each rate represents the mean of three experiments at each voltage. The dotted line is a Boltzmann function fit to the relative open probabilities. There is little difference between Cd^{2+} blocked and unblocked 464C channels in the voltage dependence of gating.

attempt to close the channels with voltage before returning to the Cd^{2+}-free control solution. If there is an intracellular gate that can close completely while Cd^{2+} is bound, then we would expect the gate could trap Cd^{2+} inside the channels, so that they remain blocked while they are held at +10 mV and unblock only after they are opened again.

The results of such a trapping experiment are shown in Fig. 7. The top trace shows the control experiment on Cd^{2+} dissociation from open channels. During a long activating pulse, Cd^{2+} is applied briefly to achieve maximal inhibition. Cd^{2+} is then washed out and replaced by an EGTA-containing solution to chelate any leftover Cd^{2+}. The recovery that ensues has a small fast component, followed by the main component of $\tau \approx 12$ s. In the bottom trace, the fast component of recovery is permitted to occur, and then the voltage is stepped to close the blocked channels. (The fast recovery is comparable in rate to channel activation, so it is not possible to test this component for trapping.) When the channels are reopened after a 30 s step to +10 mV, almost no additional recovery has occurred. This indicates that Cd^{2+} was trapped in the closed channels.

The properties of Cd^{2+} blockade in the 464C mutant provide strong evidence for a gate at the intracellular entrance to the pore in spHCN channels. For additional insight into the geography of gating, we looked at the properties of three other mutants that were strongly inhibited by Cd^{2+}.

DISCUSSION

HCN Channels Appear to Have an Intracellular Gate like Kv Channels

The crystal structure of the bacterial KcsA channel pore reveals two regions with the potential to serve as a gate for permeant ions: a GYG-containing selectivity filter, located extracellular to the central pore cavity, and a crossing bundle of pore-lining helices, forming the intracellular end of the cavity (Doyle et al., 1998). Functional studies aimed at distinguishing between these possibilities have so far indicated that the role of these two structures in gating may be different even in related channels. The *Shaker* voltage-activated K channel appears to gate at the intracellular entrance to the pore; closing this gate with hyperpolarization can prevent pore access to small MTS reagents (Liu et al., 1997) and metal cations like Cd^{2+}

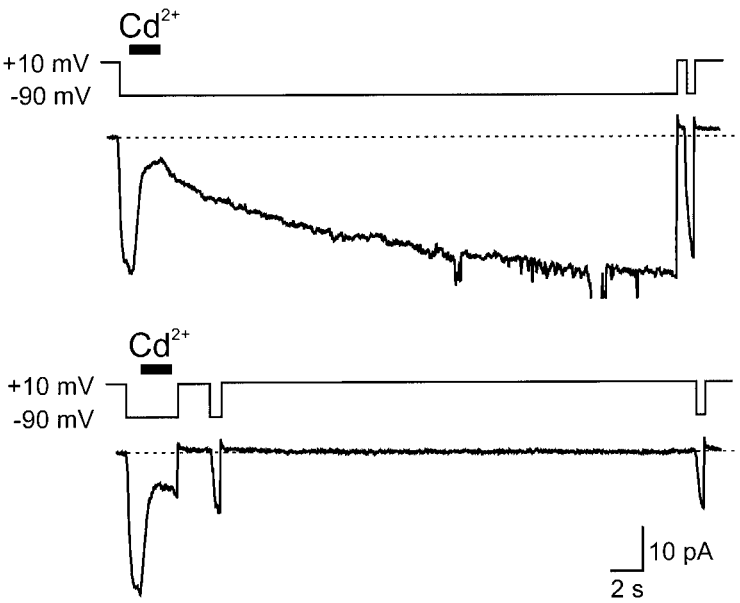

FIGURE 7. Cd^{2+} can be trapped in closed TC/TC channels. Current from an inside-out patch containing TC/TC channels, which contain cysteines at 464 in two of four subunits (see RESULTS and Fig. 4 A). In the top trace, channels were held open at −90 mV and blocked with Cd^{2+} (20 μM, horizontal bar). Cd^{2+} was removed, and the current recovered over the next 30 s. A subsequent test pulse (500 ms at −90 mV) shows activation of the recovered channels. In the bottom trace, channels were held open at −90 mV and blocked with the same concentration of Cd^{2+}. After allowing for a fast component of recovery (RESULTS), a brief test pulse (500 ms at −90 mV) was given to measure the initial level of block. We attempted to hold the channels closed at +10 mV for 30 s. A subsequent test pulse showed that almost no recovery occurred after the initial test pulse, indicating that Cd^{2+} had been trapped.

and Ag^+ (del Camino and Yellen, 2001), applied from the intracellular side. In contrast, intracellular Ag^+ can modify CNG channels equally well in either the open or closed state (Flynn and Zagotta, 2001).

Although HCN channels have structural elements in common with both *Shaker* (six transmembrane regions, strongly charged S4, GYG sequence in selectivity filter) and with CNG channels (nucleotide binding domain), our results indicate that HCN channels may be gated strongly at the intracellular entrance to the pore, like *Shaker*. In our studies, HCN channels were opened and closed by voltage and not by nucleotide. Since voltage sensor movements and the movements induced by nucleotide binding may be quite different, these different activation modalities may affect gating changes in different parts of the pore. Since spHCN channels are themselves gated by cAMP, it will be important to examine whether a different voltage- and ligand gate operates within this single species of channel.

Although technical difficulties (del Camino and Yellen, 2001) so far have precluded the use of Ag^+ for our studies on HCN channels, the use of Cd^{2+} as a gating probe, with the spHCN mutant T464C to report Cd^{2+} access, is likely to have been a valid indicator of the location of the gate. The ionic radius of Cd^{2+} is small (97 pm), similar to that of Na^+ (95 pm) and smaller than that of K^+ (133 pm); thus, a gate that can prevent Cd^{2+} entry to the pore also may prevent the entry of permeant ions. High affinity binding sites for Cd^{2+} tend to require the close proximity of several sulfhydryl groups.[1] The cysteines introduced at spHCN position 464 appear to form such a binding site. They are located in the pore-lining S6 helices. When 464C is present in all four subunits, Cd^{2+} can block the current irreversibly. When 464C is present in only two out of four subunits, Cd^{2+} can still block, but not irreversibly, indicating a reduced affinity. When 464C is absent (i.e., in wild-type spHCN), Cd^{2+} does not block. Finally, the gating of the 464C mutant appears very similar to that of wild-type spHCN. Although Cd^{2+} itself is not a permeant ion for these channels, its small size combined with its favorable chemistry render it a viable gating probe.

Cd^{2+} Bound Channels Appear to Have a Functional Voltage Sensor and Gate

Cd^{2+} inhibition of the 464C mutant could result either from a direct obstruction of the conduction pathway by Cd^{2+} or from Cd^{2+} binding outside of the conduction pathway that locks the gate closed. Two lines of evidence suggest that the gate of the 464C channels is not locked closed by Cd^{2+}, but rather continues to open and close in response to voltage. First, the recovery of Cd^{2+}-blocked channels in the presence of DMPS is much slower at depolarized voltages that should close the channel (Fig. 5). Similarly, the release of Cd^{2+} from channels containing only two 464C subunits is prevented by depolarization (Fig. 7). It also appears that the voltage sensors of Cd^{2+}-bound channels are functional because the recovery rate of 464C current with DMPS shows a voltage dependence similar to that of gating (Fig. 6). Finally, it seems that movement of the gate and voltage sensor might not involve a very large obligatory movement of the Cd^{2+} bound 464C residues because the inferred gating of Cd^{2+}-bound 464C channels is not strongly shifted along the voltage axis (Fig. 6).

All of these properties of Cd^{2+} blockade and recovery in the spHCN 464C mutant are strikingly similar to the *Shaker* mutant V474C (Liu et al., 1997). It seems likely that spHCN T464 and *Shaker* V474 both face the center of the pore in these channels. However, sequence alignment of the S6 regions of these two channels suggests that spHCN T464 is actually the homologue of *Shaker* V478, which shows reversible Cd^{2+} inhibition and only weakly gated access even to large sulfhydryl reagents (Liu et al., 1997; del Camino and Yellen, 2001). So even though Cd^{2+} can block current in cysteine mutants of both channels, the detailed structure, and, in particular, the point at which the S6 helices converge to form the "bundle crossing," is probably different. It will be interesting to learn if this different configuration is related to the inverted voltage dependence of HCN channels.

We thank Dr. U. Benjamin Kaupp for the spHCN clone. We are grateful to Tatiana Abramson for expert technical assistance and to Donato del Camino, Sarah Webster, and John Dekker for helpful discussions.

This work was supported by a National Institutes of Health research grant to G. Yellen (No. HL57383) and the McKnight Endowment Fund for Neuroscience.

Submitted: 30 October 2001
Revised: 30 November 2001
Accepted: 3 December 2001

[1]The requirement of sulfhydryl proximity for tight Cd^{2+} binding is a likely explanation for the relatively low on-binding rate for Cd^{2+} in HCN channels (3.7×10^5 $M^{-1}s^{-1}$ versus a diffusion-limited rate of $\sim 10^9$ $M^{-1}s^{-1}$). Presumably, the irreversible Cd^{2+} binding we monitor requires a very rapid, low affinity encounter of Cd^{2+} with a single sulfhydryl, followed by motion of other nearby sulfhydryls leading to irreversible Cd^{2+} trapping. Other factors (electrostatic and steric) also will help determine the binding rate. It is worth noting that the rate constant measured here is comparable to the Cd^{2+} on-rate constant for the *Shaker* V474C mutant (3.8×10^5 $M^{-1}s^{-1}$; del Camino and Yellen, 2001).

REFERENCES

Ausubel, F.M., R. Brent, R.E. Kingston, D.D. Moore, J.G. Seidman, J.A. Smith, and K. Struhl. 1996. Current Protocols in Molecular Biology. John Wiley & Sons Inc., New York. Section 8.5.

Brown, H., and D. DiFrancesco. 1980. Voltage-clamp investigations of membrane currents underlying pace-maker activity in rabbit sinoatrial node. *J. Physiol.* 308:331–351.

Brown, H.F., D. DiFrancesco, and S.J. Noble. 1979. How does adrenaline accelerate the heart? *Nature.* 280:235–236.

Chen, S., J. Wang, and S.A. Siegelbaum. 2001a. Properties of hyperpolarization-activated pacemaker current defined by coassembly of HCN1 and HCN2 subunits and basal modulation by cyclic nucleotide. *J. Gen. Physiol.* 117:491–503.

Chen, J., J.S. Mitcheson, M. Tristani-Firouzi, M. Lin, and M.C. Sanguinetti. 2001b. The S4-S5 linker couples voltage sensing and activation of pacemaker channels. *Proc. Natl. Acad. Sci. USA.* 98: 11277–11282.

del Camino, D., and G. Yellen. 2001. Tight steric closure at the intracellular activation gate of a voltage-gated K^+ channel. *Neuron.* 32:649–656.

DiFrancesco, D. 1993. Pacemaker mechanisms in cardiac tissue. *Annu. Rev. Physiol.* 55:455–472.

DiFrancesco, D., and P. Tortora. 1991. Direct activation of cardiac pacemaker channels by intracellular cAMP. *Nature.* 351:145–147.

Doyle, D.A., J. Morais-Cabral, R.A. Pfuetzner, A. Kuo, J.M. Gulbis, S.L. Cohen, B.T. Chait, and R. MacKinnon. 1998. The structure of the potassium channel: molecular basis of potassium conduction and selectivity. *Science.* 280:69–77.

Flynn, G.E., and W.N. Zagotta. 2001. Conformational changes in S6 coupled to the opening of cyclic nucleotide-gated channels. *Neuron.* 30:689–698.

Gauss, R., R. Seifert, and U.B. Kaupp. 1998. Molecular identification of a hyperpolarization-activated cation channel in sea urchin sperm. *Nature.* 393:583–587.

Hamill, O.P., A. Marty, E. Neher, B. Sakmann, and F.J. Sigworth. 1981. Improved patch-clamp techniques for high-resolution current recording from cells and cell-free membrane patches. *Pflügers Arch.* 391:85–100.

Holmgren, M., K.S. Shin, and G. Yellen. 1998. The activation gate of a voltage-gated K^+ channel can be trapped in the open state by an intersubunit metal bridge. *Neuron.* 21:617–621.

Jurman, M.E., L.M. Boland, Y. Liu, and G. Yellen. 1994. Visual identification of individual transfected cells for electrophysiology using antibody-coated beads. *Biotechniques.* 17:876–881.

Liu, Y., M. Holmgren, M.E. Jurman, and G. Yellen. 1997. Gated access to the pore of a voltage-dependent K+ channel. *Neuron.* 19: 175–184.

Ludwig, A., X. Zong, M. Jeglitsch, F. Hofmann, and M. Biel. 1998. A family of hyperpolarization-activated mammalian cation channels. *Nature.* 393:587–591.

Pape, H.C. 1996. Queer current and pacemaker: the hyperpolarization-activated cation current in neurons. *Annu. Rev. Physiol.* 58: 299–327.

Pape, H.C., and D.A. McCormick. 1989. Noradrenaline and serotonin selectively modulate thalamic burst firing by enhancing a hyperpolarization-activated cation current. *Nature.* 340:715–718.

Rothberg, B.S., K.S. Shin, P. Phale, and G. Yellen. 2001. Gated access to the pore of a hyperpolarization-activated cation channel. *Biophys. J.* 80:16A (Abstr.).

Santoro, B., D.T. Liu, H. Yao, D. Bartsch, E.R. Kandel, S.A. Siegelbaum, and G.R. Tibbs. 1998. Identification of a gene encoding a hyperpolarization-activated pacemaker channel of brain. *Cell.* 93: 717–729.

Seed, B., and A. Aruffo. 1987. Molecular cloning of the CD2 antigen, the T-cell erythrocyte receptor, by a rapid immunoselection procedure. *Proc. Natl. Acad. Sci. USA.* 84:3365–3369.

Shin, K.S., B.S. Rothberg, and G. Yellen. 2001. Blocker state dependence and trapping in hyperpolarization-activated cation channels: evidence for an intracellular activation gate. *J. Gen. Physiol.* 117:91–101.

Yellen, G. 1998. The moving parts of voltage-gated ion channels. *Q. Rev. Biophys.* 31:239–296.